CLEO CONF 95-10
EPS0166
July 24, 1995

Measurement of $\mathcal{B}(B^- \to D^0 \ell^- \bar{\nu})$ Using Neutrino Reconstruction Techniques

Y. Kubota,[1] M. Lattery,[1] M. Momayezi,[1] J.K. Nelson,[1] S. Patton,[1] R. Poling,[1] V. Savinov,[1] S. Schrenk,[1] R. Wang,[1] M.S. Alam,[2] I.J. Kim,[2] Z. Ling,[2] A.H. Mahmood,[2] J.J. O'Neill,[2] H. Severini,[2] C.R. Sun,[2] F. Wappler,[2] G. Crawford,[3] R. Fulton,[3] D. Fujino,[3] K.K. Gan,[3] K. Honscheid,[3] H. Kagan,[3] R. Kass,[3] J. Lee,[3] M. Sung,[3] C. White,[3] A. Wolf,[3] M.M. Zoeller,[3] X. Fu,[4] B. Nemati,[4] W.R. Ross,[4] P. Skubic,[4] M. Wood,[4] M. Bishai,[5] J. Fast,[5] E. Gerndt,[5] J.W. Hinson,[5] T. Miao,[5] D.H. Miller,[5] M. Modesitt,[5] E.I. Shibata,[5] I.P.J. Shipsey,[5] P.N. Wang,[5] L. Gibbons,[6] S.D. Johnson,[6] Y. Kwon,[6] S. Roberts,[6] E.H. Thorndike,[6] T.E. Coan,[7] J. Dominick,[7] V. Fadeyev,[7] I. Korolkov,[7] M. Lambrecht,[7] S. Sanghera,[7] V. Shelkov,[7] T. Skwarnicki,[7] R. Stroynowski,[7] I. Volobouev,[7] G. Wei,[7] M. Artuso,[8] M. Gao,[8] M. Goldberg,[8] D. He,[8] N. Horwitz,[8] S. Kopp,[8] G.C. Moneti,[8] R. Mountain,[8] F. Muheim,[8] Y. Mukhin,[8] S. Playfer,[8] S. Stone,[8] X. Xing,[8] J. Bartelt,[9] S.E. Csorna,[9] V. Jain,[9] S. Marka,[9] D. Gibaut,[10] K. Kinoshita,[10] P. Pomianowski,[10] B. Barish,[11] M. Chadha,[11] S. Chan,[11] D.F. Cowen,[11] G. Eigen,[11] J.S. Miller,[11] C. O'Grady,[11] J. Urheim,[11] A.J. Weinstein,[11] F. Würthwein,[11] D.M. Asner,[12] M. Athanas,[12] D.W. Bliss,[12] W.S. Brower,[12] G. Masek,[12] H.P. Paar,[12] J. Gronberg,[13] C.M. Korte,[13] R. Kutschke,[13] S. Menary,[13] R.J. Morrison,[13] S. Nakanishi,[13] H.N. Nelson,[13] T.K. Nelson,[13] C. Qiao,[13] J.D. Richman,[13] D. Roberts,[13] A. Ryd,[13] H. Tajima,[13] M.S. Witherell,[13] R. Balest,[14] K. Cho,[14] W.T. Ford,[14] M. Lohner,[14] H. Park,[14] P. Rankin,[14] J.G. Smith,[14] J.P. Alexander,[15] C. Bebek,[15] B.E. Berger,[15] K. Berkelman,[15] K. Bloom,[15] T.E. Browder,[15,a] D.G. Cassel,[15] H.A. Cho,[15] D.M. Coffman,[15] D.S. Crowcroft,[15] M. Dickson,[15] P.S. Drell,[15] D.J. Dumas,[15] R. Ehrlich,[15] R. Elia,[15] P. Gaidarev,[15] M. Garcia-Sciveres,[15] B. Gittelman,[15] S.W. Gray,[15] D.L. Hartill,[15] B.K. Heltsley,[15] S. Henderson,[15] C.D. Jones,[15] S.L. Jones,[15] J. Kandaswamy,[15] N. Katayama,[15] P.C. Kim,[15] D.L. Kreinick,[15] T. Lee,[15] Y. Liu,[15] G.S. Ludwig,[15] J. Masui,[15] J. Mevissen,[15] N.B. Mistry,[15] C.R. Ng,[15] E. Nordberg,[15] J.R. Patterson,[15] D. Peterson,[15] D. Riley,[15] A. Soffer,[15] P. Avery,[16] A. Freyberger,[16] K. Lingel,[16] C. Prescott,[16] J. Rodriguez,[16] S. Yang,[16] J. Yelton,[16] G. Brandenburg,[17] D. Cinabro,[17] T. Liu,[17] M. Saulnier,[17] R. Wilson,[17] H. Yamamoto,[17] T. Bergfeld,[18] B.I. Eisenstein,[18] J. Ernst,[18] G.E. Gladding,[18] G.D. Gollin,[18] M. Palmer,[18] M. Selen,[18] J.J. Thaler,[18] K.W. Edwards,[19] K.W. McLean,[19] M. Ogg,[19] A. Bellerive,[20] D.I. Britton,[20] E.R.F. Hyatt,[20] R. Janicek,[20] D.B. MacFarlane,[20] P.M. Patel,[20] B. Spaan,[20] A.J. Sadoff,[21] R. Ammar,[22] P. Baringer,[22] A. Bean,[22] D. Besson,[22] D. Coppage,[22] N. Copty,[22] R. Davis,[22] N. Hancock,[22] S. Kotov,[22] I. Kravchenko,[22] and N. Kwak[22]

(CLEO Collaboration)

[1] University of Minnesota, Minneapolis, Minnesota 55455
[2] State University of New York at Albany, Albany, New York 12222
[3] Ohio State University, Columbus, Ohio, 43210
[4] University of Oklahoma, Norman, Oklahoma 73019
[5] Purdue University, West Lafayette, Indiana 47907
[6] University of Rochester, Rochester, New York 14627
[7] Southern Methodist University, Dallas, Texas 75275
[8] Syracuse University, Syracuse, New York 13244
[9] Vanderbilt University, Nashville, Tennessee 37235
[10] Virginia Polytechnic Institute and State University, Blacksburg, Virginia, 24061
[11] California Institute of Technology, Pasadena, California 91125
[12] University of California, San Diego, La Jolla, California 92093
[13] University of California, Santa Barbara, California 93106
[14] University of Colorado, Boulder, Colorado 80309-0390
[15] Cornell University, Ithaca, New York 14853
[16] University of Florida, Gainesville, Florida 32611
[17] Harvard University, Cambridge, Massachusetts 02138
[18] University of Illinois, Champaign-Urbana, Illinois, 61801
[19] Carleton University, Ottawa, Ontario K1S 5B6 and the Institute of Particle Physics, Canada
[20] McGill University, Montréal, Québec H3A 2T8 and the Institute of Particle Physics, Canada
[21] Ithaca College, Ithaca, New York 14850
[22] University of Kansas, Lawrence, Kansas 66045

Abstract

We present a new measurement of the branching fraction $\mathcal{B}(B^- \to D^0\ell^-\bar{\nu})$. $B^- \to D^0\ell^-\bar{\nu}$ decays are identified via full reconstruction, using a measurement of the missing energy and momentum to infer the neutrino momentum. Based on 2.46 fb^{-1} of data taken with the CLEO detector at CESR, we find $\mathcal{B}(B^- \to D^0\ell^-\bar{\nu}) = (1.95 \pm 0.29 \pm 0.47)\%$ in the ISGW model, where the first error is statistical and the second is systematic.

1 Introduction

Recent measurements [1] of the B meson semileptonic branching fraction indicate a lower value of this quantity than is predicted by a number of theoretical calculations [2]. Thus, it is important to account for the various final states that contribute to the semileptonic decay rate. The decay $B \to D^*\ell\nu$ is known to contribute about half of the semileptonic rate [3], but little is known about the other exclusive decay rates. In addition, it is important to study the distribution of q^2, the invariant mass squared of the lepton-neutrino system in semileptonic decays, since it is sensitive to the decay form factors.

In this paper, we present a new value of the branching fraction $\mathcal{B}(B^- \to D^0\ell^-\bar{\nu})$. Our measurement uses the technique of neutrino reconstruction to identify $B^- \to D^0\ell^-\bar{\nu}$ decays, and to suppress backgrounds from $B \to D^*\ell\nu$ and semileptonic decays to other D resonances. By measuring the four-momentum of the neutrino produced in the decay, we are able to fully reconstruct the B meson. This technique has recently been used in a measurement of the $B \to \pi\ell\nu$ branching fraction [4]. Because of the strength of the background suppression, kinematic cuts are not required to isolate the signal events, and we can to examine the q^2 distribution for the decay. Below, we describe the experimental environment, the reconstruction of $B^- \to D^0\ell^-\bar{\nu}$ decays, the treatment of the backgrounds, and the extraction of $\mathcal{B}(B^- \to D^0\ell^-\bar{\nu})$.

2 Experimental Method

Our data sample consists of 2.63×10^6 $B\bar{B}$ pairs which are produced in e^+e^- collisions at the $\Upsilon(4S)$ resonance, corresponding to an integrated luminosity of 2.46 fb^{-1}, collected by the CLEO detector at the Cornell Electron Storage Ring (CESR). In this environment, the $B\bar{B}$ system is at rest, and the B meson energy is the same as the beam energy E_{beam}. We assume equal production of B^+B^- and $B^0\bar{B}^0$ from the $\Upsilon(4S)$. The detector is described in detail elsewhere [5], but for this analysis we note that it has excellent hermeticity and angular coverage. Three concentric tracking devices provide a momentum resolution of $\sigma_p/p = 0.005 \oplus 0.0015p$ (p in GeV/c), while covering 95% of the 4π solid angle. The CsI calorimeter located inside of the CLEO solenoid provides an energy resolution well approximated by $\sigma_E/E = 0.019 + 0.0035/E^{0.75} - 0.001E$ (E in GeV), while covering 98% of 4π.

For this analysis we select hadronic events that have at least one track identified as a lepton. In order to suppress events from continuum production of quark-antiquark pairs, we require that the ratio of the Fox-Wolfram [9] moments, H_2/H_0, be less than 0.4. Electrons are identified through specific ionization, energy and momentum measurements, and position matching between the tracking and calorimeter systems. We accept electron candidates with momenta greater than 0.8 GeV/c, and that fall within the region $|\cos\theta_e| < 0.91$, where θ_e is the angle of the electron candidate direction with respect to the beam axis. Muons are identified through hits in muon counters at a depth of five interaction lengths, limiting muon candidates to momenta greater than 1.4 GeV/c, and to the region $|\cos\theta| < 0.87$.

We search for D^0 candidates in the decay mode $D^0 \to K^-\pi^+$. Kaons and pions are unambiguously chosen by charge correlation with the lepton (the kaon and lepton must have the same sign). D^0 candidates are required to have an invariant mass of $1.85 \leq M_{K\pi} \leq 1.88$ GeV. Since the D^0 must come from a B decay, we also require $|\vec{p}_{K\pi}|/\sqrt{(E_{beam}^2 - M_{K\pi}^2)} < 0.5$.

For this analysis, we wish to eliminate any D^0 candidates that are daughters of D^* decays. In each event the candidate D^0 is paired with charged pions, neutral pions, and photons to form candidate D^* mesons. If the candidate $D^* - D$ mass difference is within 4 MeV for charged pions, 3 MeV for neutral pions, and 6 MeV for photons of the nominal $D^* - D$ mass difference, we veto the event.

We select D^0 – lepton pairs that are consistent with $B^- \to D^0\ell^-\bar{\nu}$ decays by taking advantage of our knowledge of the B meson momentum, $|\vec{p}_B|$. As noted previously, for B mesons produced in e^+e^- annihilations at the $\Upsilon(4S)$ energy, the B meson energy, E_B, must be equal to the beam energy which is precisely known; hence $|\vec{p}_B|$ can be determined from E_B and the known B mass [7]. We define the quantity

$$\cos\theta_{BZ} = \frac{|\vec{p}_Z|^2 + |\vec{p}_B|^2 - |E_B - E_Z|^2}{2|\vec{p}_B||E_B - E_Z|},$$

where E_Z and $\vec{p}_Z$ are the energy and momentum of the $D^0 - \ell$ system. For true $B^- \to D^0\ell^-\bar{\nu}$ decays, $\cos\theta_{BZ}$ will correspond to the cosine of the angle between the B meson three-momentum and the three-momentum of the $D^0 - \ell$ system, and will have a physical value, *i.e.*, it will fall between -1 and 1. For decays in which a pion or photon from the B decay chain is missing (*e.g.* $B \to D^*\ell\nu$ decays where the extra pion or photon from the D^* decay is lost), $\cos\theta_{BZ}$ need not have physical values. $D^0 - \ell$ pairs are required to have $\cos\theta_{BZ}$ values between -1 and 1. This cut further supresses the dominant background to this analysis from semileptonic B decays to excited charm final states.

Neutrinos can only be identified indirectly. In this analysis, we reconstruct the neutrino four-momentum by measuring the momentum and energy missing from each event. We define

$$\begin{aligned} E_{miss} &\equiv 2E_{beam} - \sum_i E_i \\ \vec{p}_{miss} &\equiv -\sum_i \vec{p}_i, \end{aligned}$$

where the index i runs over all legitimate charged tracks and calorimeter showers. To obtain an accurate measurement of E_{miss} and $\vec{p}_{miss}$, we have developed algorithms to reject fake tracks and clusters from the events. Good resolution for the unobserved neutrino can only be achieved in events with very few missing particles. Therefore, we make requirements on event quality to remove events with missing particles in addition to the neutrino. We remove events with more than one lepton, since they indicate additional missing neutrinos. We also make a requirement on the net charge of the event. Only events with net charge of 0 or ± 1 are used, with the additional restriction that events with net charge equal to the lepton charge are removed. This latter restriction is to further eliminate events with $\bar{B}^0 \to D^{*+}\ell^-\bar{\nu}$ decays, where $D^{*+} \to D^0\pi^+$. For these decays, the π^+ from the D^{*+} decay has momentum less than 225 MeV/c. Since track finding is inefficient at low momentum, this positively charged pion is often lost. Thus, we remove events with negatively charged leptons that have a negative net charge.

Events with other missing particles, such as K_L^0 mesons, are eliminated by requiring that the missing mass in the event, $MM^2 \equiv E_{miss}^2 - |\vec{p}_{miss}|^2$, be consistent with zero. We

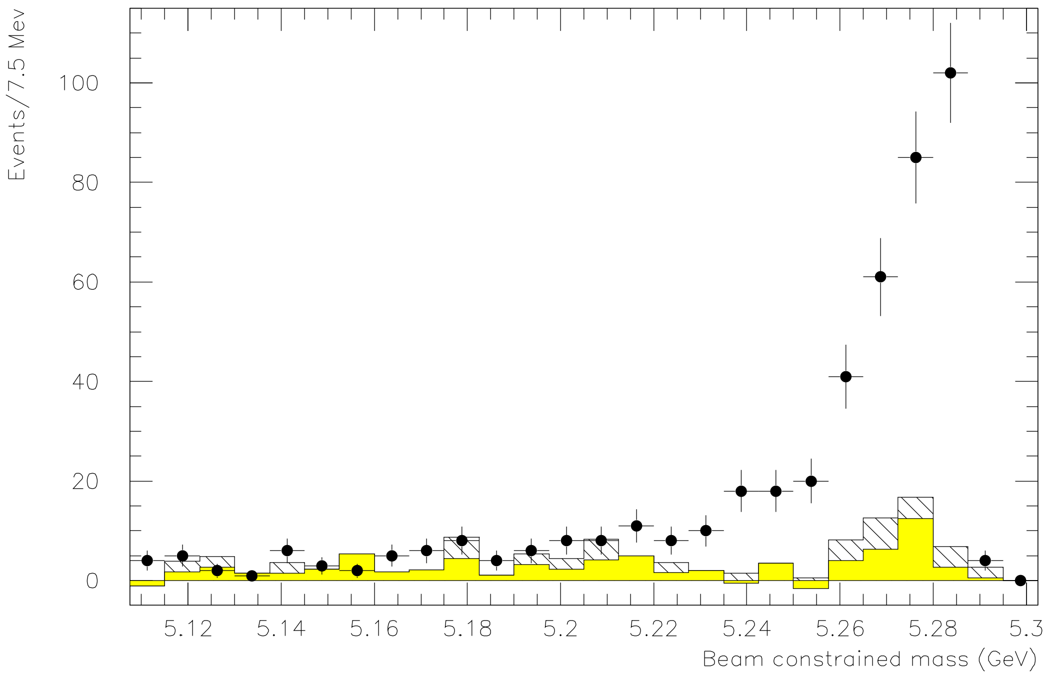

Figure 1: Beam constrained mass spectrum for candidate $B^- \to D^0\ell^-\bar{\nu}$ events. The hatched area represents the background due to events from the continuum, and the shaded area represents the combinatoric background. The peak still includes some events from $B \to D^*\ell\nu$ and $B \to D^{**}\ell\nu$ decays.

require $-450 \leq MM^2/2E_{miss} \leq 300$ MeV, since the resolution on MM^2 varies roughly as $2E_{miss}\sigma_{E_{miss}}$. We have achieved resolutions of approximately 260 MeV on E_{miss} and 110 MeV/c on $\vec{p}_{miss}$ in events that do not contain K_L^0 particles or additional neutrinos.

$B^- \to D^0\ell^-\bar{\nu}$ candidates are selected through a full reconstruction of the B. The energy difference $\Delta E \equiv E_{beam} - (E_{D^0} + E_\ell + |\vec{p}_{miss}|)$ should be zero, and the beam constrained mass $M_B \equiv \sqrt{E_{beam}^2 - |\vec{p}_{D^0} + \vec{p}_\ell + \vec{p}_{miss}|^2}$ should be equal to the B mass. In this analysis, we require $-500 \leq \Delta E \leq 100$ MeV. The ΔE cut is asymmetric because of $B \to D^*\ell\nu$ backgrounds that are present at higher ΔE. Figure 1 shows the beam constrained mass distribution for events passing all of the above cuts. The signal region is $5.2650 \leq M_B < 5.2875$ GeV. The yield in the signal region is 248 events.

3 Backgrounds, Yields, and Efficiencies

While there is a significant enhancement near the B mass in Figure 1, there are still substantial backgrounds to be considered. One source of background is $D^0-\ell^-$ pairs from continuum production of quark-antiquark pairs. These events are represented using data taken at center of mass energies below the $\Upsilon(4S)$ resonance and the scaled B mass distribution for these continuum events is shown as the hatched area in Figure 1.

Another background in this analysis is the combinatoric background in the D^0 reconstruction. This background is well modeled by events passing all other analysis cuts but where the D^0 candidate mass is just outside the D^0 mass cuts. We select $1.78 \leq M_{K\pi} < 1.83$ GeV and $1.90 \leq M_{K\pi} < 1.95$ GeV for the sideband region. The scaled B mass distribution for events in the D^0 sideband region, where the continuum contribution has been subtracted, is shown as the shaded area in Figure 1.

The most important background in this analysis arises from semileptonic decays to excited D mesons. $B \to D^{*(*)}\ell\nu$ decays are very similar to $B^- \to D^0\ell^-\bar{\nu}$ decays in their kinematics. In particular, because the $D^* - D$ mass difference is so small, $B \to D^*\ell\nu$ events reconstructed as $B^- \to D^0\ell^-\bar{\nu}$ are only slightly smeared in M_B, and slightly shifted in ΔE compared to true $B^- \to D^0\ell^-\bar{\nu}$ events. All D^{*0} mesons and 68% of $D^{*\pm}$ mesons decay to a D^0, so it is important to understand this background.

The contribution to the yield from $B \to D^*\ell\nu$ decays is modeled by Monte Carlo simulation, and is normalized to the measured CLEO branching fractions for $B \to D^*\ell\nu$ [3]: $\mathcal{B}(\bar{B}^0 \to D^{*+}\ell^-\nu) = (4.49 \pm 0.32 \pm 0.39)\%$ and $\mathcal{B}(B^- \to D^{*0}\ell^-\nu) = (5.13 \pm 0.54 \pm 0.64)\%$. The estimated yields in the signal region due to these decays are given in Table 1. The error on the yields is included in the summary of systematic errors. The contributions from the $B \to D^{**}\ell\nu$ decays are subtracted in a similar way. We assume that 2.5% of B mesons decay to the narrow D^{**} states D_1 and D_2^*, and 1.1% of B mesons decay to broad $D\pi$ and $D^*\pi$ final states. The branching fractions for the various $B \to D^{**}\ell\nu$ are not well known, so we attribute a large uncertainty to their contribution, which will be included in the systematic error. However, because the decay kinematics are sufficiently different from $B^- \to D^0\ell^-\bar{\nu}$, this contribution is relatively small.

Finally, there are backgrounds due to uncorrelated events, in which the lepton and D^0 are daughters of different B's, and due to fake leptons. These backgrounds are very small, and they are not subtracted explicitly but instead included in our estimate of the systematic error.

Table 1 gives the numbers of events in our data sample passing all of the cuts described above, and our estimates of the various backgrounds. Figure 2 shows the B mass spectrum with the contributions from the D^0 sideband and the continuum subtracted. The histograms indicate the contributions from the $B \to D^{*(*)}\ell\nu$ decays. As described, the various excited D backgrounds are smeared out in M_B compared to the signal. Figure 2 shows the ΔE distribution for events in the M_B signal region; again, the histograms indicate the contributions from the $B \to D^{*(*)}\ell\nu$ decays. The backgrounds have larger values of ΔE compared to the signal. Figure 3 shows the M_B distribution after all background subtractions. We find $N_{D^0\ell^-\bar{\nu}} = 117.7 \pm 17.3$ events remain within the signal region, $5.2650 \leq M_B < 5.2875$ GeV. Figure 3 also shows the M_B distribution from the Monte Carlo simulation of $B^- \to D^0\ell^-\bar{\nu}$ decays, normalized to equal area in the signal region.

We have studied various kinematic distributions for the signal events to see that they

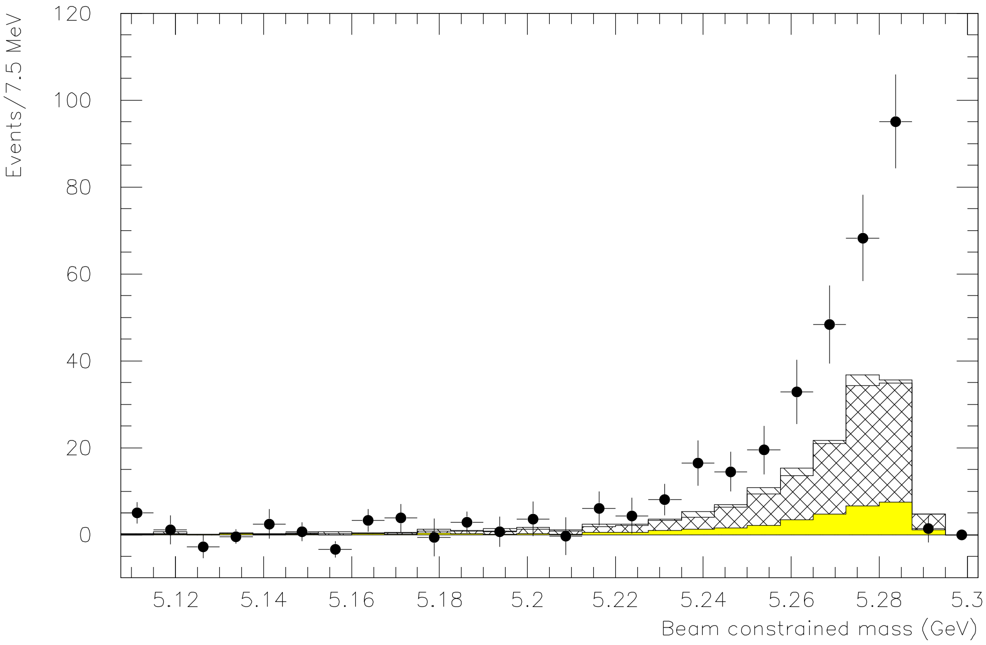

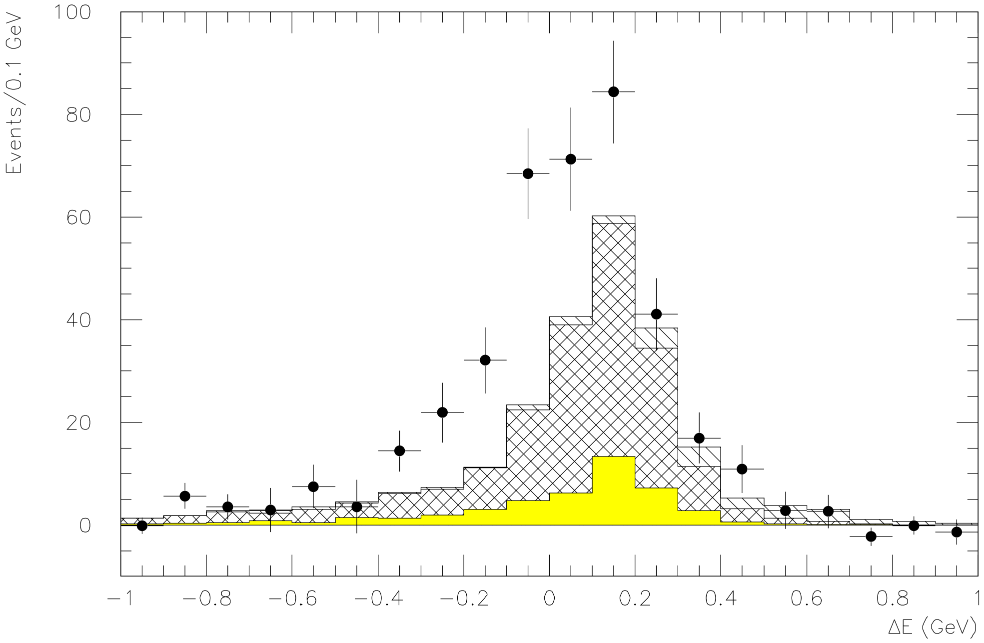

Figure 2: Beam constrained mass spectrum (top) and ΔE distribution (bottom) after continuum and sideband subtraction. The shaded area represents the contribution from $\bar{B}^0 \to D^{*+}\ell^-\nu$ events, the cross-hatched area represents the contribution from $B^- \to D^{*0}\ell^-\bar{\nu}$ events, and the hatched area represents the contribution from $B \to D^{**}\ell\nu$ events. Events in the top plot have $-500 \leq \Delta E \leq 100$ MeV, and events in the bottom plot have $5.2650 \leq M_B < 5.2875$ GeV.

Table 1: Signal and background yields. The errors on the background yields are included in the summary of systematic errors; errors are statisitcal only.

Yields	On $\Upsilon(4S)$	Off $\Upsilon(4S)$	From $B\bar{B}$ decays		
D^0 signal	248	7	233.3	$\pm$	16.8
Scaled D^0 sideband	35.4	6.6	21.5	$\pm$	4.4
Signal - sideband			211.8	$\pm$	17.3
$(\bar{B}^0 \to D^{*+}\ell^-\bar{\nu})(D^{*+} \to D^0\pi^+)$			18.8		
$(B^- \to D^{*0}\ell^-\bar{\nu})(D^{*0} \to D^0\pi^0)$			45.5		
$(B^- \to D^{*0}\ell^-\bar{\nu})(D^{*0} \to D^0\gamma)$			25.8		
$B \to D^{**}\ell\nu$			4.0		
$B^- \to D^0\ell^-\bar{\nu}$			117.7	$\pm$	17.3

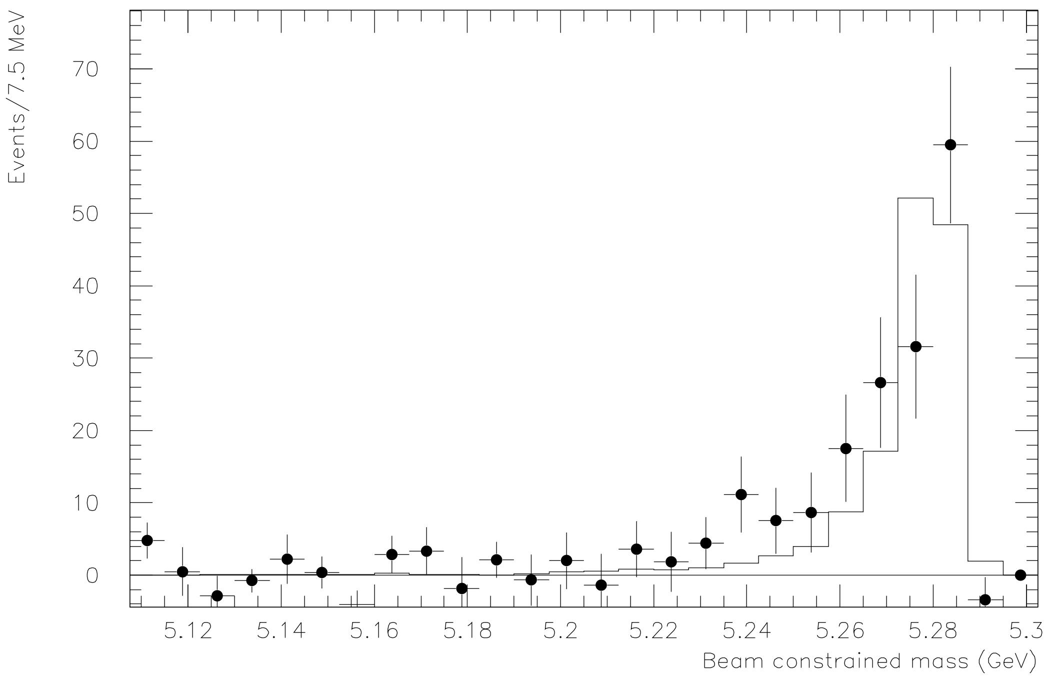

Figure 3: Beam constrained mass spectrum after all background subtractions. The error bars are statistical only. The histogram is the predicted spectrum from signal Monte Carlo, normalized to equal area in the signal region, $5.2650 \leq M_B < 5.2875$ GeV.

Table 2: Systematic errors on $\mathcal{B}(B^- \to D^0 \ell^- \bar{\nu})\mathcal{B}(D^0 \to K^- \pi^+)$

Source	Fractional Error
Neutrino detection	20.0%
$D^* \ell \nu$ branching fractions	10.4%
Lepton veto	4.5%
Lepton fakes	2.5%
Uncorrelated background	2.5%
Lepton finding	2.0%
Luminosity	2.0%
$B \to D^{**} \ell \nu$	1.4%
Total	23.5%

are consistent with $B^- \to D^0 \ell^- \bar{\nu}$ decays, and inconsistent with the dominant $B \to D^* \ell \nu$ background. In particular, the distributions of q^2 and $\cos\theta^*_{D\ell}$, where $(\pi - \theta^*_{D\ell})$ is the angle between the D^0 and the lepton in the rest frame of the virtual W, are quite distinctive. Because $B^- \to D^0 \ell^- \bar{\nu}$ is a pseudoscalar-to-pseudoscalar decay, $\cos\theta^*_{D\ell}$ is expected to have a $\sin^2\theta$ distribution. We also note that the q^2 distribution of $B^- \to D^0 \ell^- \bar{\nu}$ decays is expected to be significantly more peaked to lower q^2 than for the $B \to D^* \ell \nu$ background, and therefore will also have a softer lepton momentum spectrum. Figure 4 shows various kinematic distributions for the data in the B mass signal region, after all backgrounds have been subtracted. These are compared to a Monte Carlo simulation of the signal distributions, and to the distributions expected from the $B \to D^* \ell \nu$ contribution. (The distributions have not been corrected for efficiencies.) One can see that the data are consistent with $B^- \to D^0 \ell^- \bar{\nu}$ decays.

The efficiency for reconstructing $B^- \to D^0 \ell^- \bar{\nu}$ decays is determined using the Monte Carlo simulation. $B^- \to D^0 \ell^- \bar{\nu}$ events are generated in the ISGW model [6] and are passed through a full detector simulation [8] and then analyzed as data. We find an efficiency for reconstructing $B^- \to D^0 \ell^- \bar{\nu}$ decays, averaged over electrons and muons, of $\epsilon_{D^0 \ell^- \bar{\nu}} = (2.93 \pm 0.01)\%$, where the error is statistical only.

The contributions to the systematic errors are listed in Table 2. The error is dominated by the uncertainties of the neutrino reconstruction procedure, and we hope to make significant progress in reducing this uncertainty in the near future. The next largest uncertainty comes from the $B \to D^* \ell \nu$ contribution. We have varied the $B \to D^* \ell \nu$ branching ratios by $\pm 1\sigma$ of their measured value, which changes the yield by 10.4%. We vary the $B \to D^{**} \ell \nu$ background by changing the model of these decays from being all narrow resonant final states (D_1 and D_2^*) to being all wide non-resonant $D\pi$ and $D^*\pi$ production, and by varying the overall normalization. This results in a 1.4% variation on the $D^0 \ell^- \bar{\nu}$ yield.

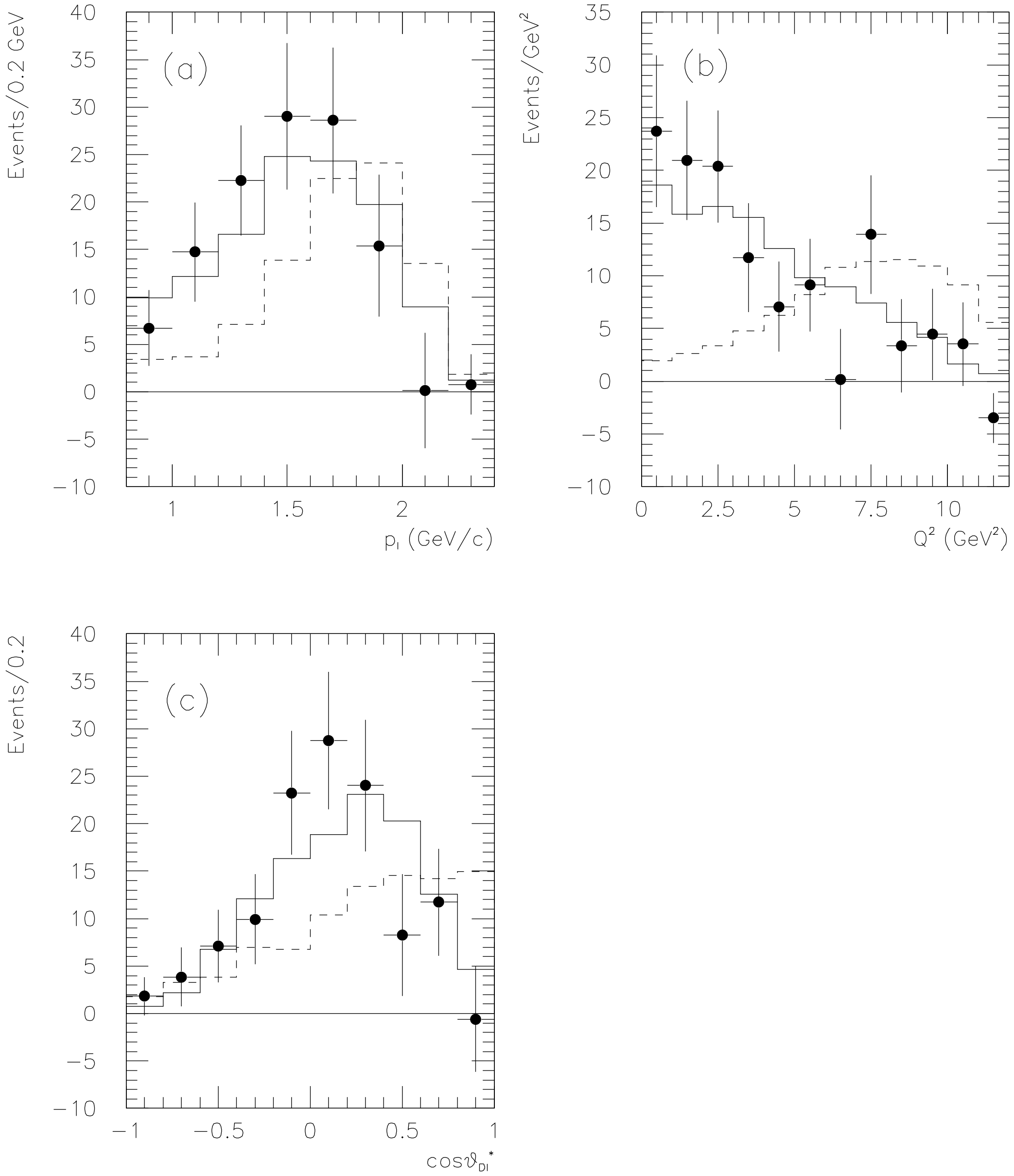

Figure 4: Kinematic distributions for the $B^- \to D^0\ell^-\bar{\nu}$ analysis: (a) lepton momentum, (b) q^2, and (c) $\cos\theta^*_{D\ell}$. The points are the distributions from the data after all backgrounds have been subtracted, the solid histograms are the predicted spectra from a Monte Carlo simulation, and the dashed histograms are the spectrum from $B \to D^*\ell\nu$ that has been subtracted. (The distributions have not been corrected for efficiencies.)

As a final check, we extract the $B^- \to D^0\ell^-\bar{\nu}$ yield by releasing the cuts on M_B and ΔE and performing a fit to the distribution of data in the $\Delta E - M_B$ plane ($5.1075 < M_B < 5.3025$ GeV, $-1.0 < \Delta E < 1.0$ GeV) to a sum of contributions from signal ($B^- \to D^0\ell^-\bar{\nu}$) and backgrounds ($B \to D^*\ell\nu$, $B \to D^{**}\ell\nu$) whose shapes in the $\Delta E - M_B$ plane are determined by Monte Carlo simulation. The resulting yield of $B^- \to D^0\ell^-\bar{\nu}$ events extracted with this method is consistent with the measured yield in the M_B signal region ($\Delta N_{D^0\ell^-\bar{\nu}}/N_{D^0\ell^-\bar{\nu}}$ = 11.8%), and furthermore the yield of $B \to D^*\ell\nu$ events that results from the fit gives $\mathcal{B}(B \to D^*\ell\nu)$ that is consistent with the measured CLEO values ($\Delta\mathcal{B}(B \to D^*\ell\nu)/\mathcal{B}(B \to D^*\ell\nu) = 0.13 \pm 0.15$).

4 Calculation of $\mathcal{B}(B^- \to D^0\ell^-\bar{\nu})$

From the efficiency and measured yields we can extract a product branching fraction

$$\mathcal{B}(B^- \to D^0\ell^-\bar{\nu})\mathcal{B}(D^0 \to K^-\pi^+) = \frac{N_{D^0\ell^-\bar{\nu}}\epsilon_{D^0\ell^-\bar{\nu}}}{4 \times N_{\Upsilon(4S)} \times f_{+-}}$$

where $N_{\Upsilon(4S)}$ is the total number of $B\bar{B}$ pairs in our data sample, $f_{+-} \equiv \mathcal{B}(\Upsilon(4S) \to B^+B^-)$ which we take to be 0.5, and the factor of 4 is because each $\Upsilon(4S)$ decays to a B meson pair and we are combining electrons and muons. We find, in the ISGW model,

$$\mathcal{B}(B^- \to D^0\ell^-\bar{\nu})\mathcal{B}(D^0 \to K^-\pi^+) = (0.0763 \pm 0.0112 \pm 0.0179)\%$$

where the first error is statistical and the second is systematic. Using the CLEO branching fraction [10]

$$\mathcal{B}(D^0 \to K^-\pi^+) = (3.91 \pm 0.19)\%,$$

this becomes

$$\mathcal{B}(B^- \to D^0\ell^-\bar{\nu}) = (1.95 \pm 0.29 \pm 0.47)\%$$

where the first error is statistical and the second is systematic. The error in the $D^0 \to K^-\pi^+$ branching fraction has been included in the systematic error, but the $K\pi$ track reconstruction uncertainty that is common to both measurements has been canceled. This results is consistent with and more precise than the only previous published measurement [11] of this branching ratio, $\mathcal{B}(B^- \to D^0\ell^-\bar{\nu}) = (1.6 \pm 0.6 \pm 0.3)\%$.

We gratefully acknowledge the effort of the CESR staff in providing us with excellent luminosity and running conditions. This work was supported by the National Science Foundation, the U.S. Department of Energy, the Heisenberg Foundation, the Alexander von Humboldt Stiftung, the Natural Sciences and Engineering Research Council of Canada, and the A.P. Sloan Foundation.

References

[a] Permanent address: University of Hawaii at Manoa.

[1] H. Albrecht *et al.*, Phys. Lett. **B318**, 397 (1993); J. Gronberg *et al.*, CLEO-CONF-94-6, paper submitted to 27th International Conference on High Energy Physics, Glasgow, Scotland, (1994).

[2] G. Altarelli and S. Petrarca, Phys. Lett. **B261**, 303 (1991); I. Bigi, B. Blok, M.A. Shifman, and A. Vainshtein, Phys. Lett. **B323**, 408 (1994).

[3] B. Barish *et al.*, Phys. Rev. **D51**, 1014 (1995).

[4] L. Gibbons, contribution to the 30th Rencontres de Moriond, "Electroweak Interactions and Unified Theories," Les Arcs, France, March 1995.

[5] Y. Kubota *et al.*, Nucl. Instrum. Methods **320**, 66 (22).

[6] N. Isgur, D. Scora, B. Grinstein, and M.B. Wise, Phys. Rev. **D39**, 799 (1989).

[7] Particle Data Group, L. Montanet *et al.*, Phys. Rev. **D50**, 1173 (1994).

[8] R. Brun *et al.*, GEANT v. 3.14, CERN Report No. CERN DD/EE/84-1 (unpublished).

[9] G. Fox and S. Wolfram, Phys. Rev. Lett. **41**, 1581 (1978).

[10] D.S. Akerib *et al.*, Phys. Rev. Lett. **69**, 3070 (1993).

[11] R. Fulton *et al.*, Phys. Rev. **D43**, 651 (1991). This result depends on previous measurements of D and D^* branching fractions which have been superceded. There is no simple way to correct this result for the new branching fractions, and therefore there is no simple way to take the average of these results.